Scientia Marina 74(3)
September 2010, 539-553, Barcelona (Spain)
ISSN: 0214-8358
doi: 10.3989/scimar.2010.74n3539

Beach cusps and inner surf zone processes: growth or destruction? A case study of Trafalgar Beach (Cádiz, Spain)

ROLAND GARNIER [1,2], MIGUEL ORTEGA-SÁNCHEZ [3], MIGUEL A. LOSADA [3], ALBERT FALQUÉS [4] and NICHOLAS DODD [1]

[1] Environmental Fluid Mechanics Research Centre, Process and Environmental Division, Faculty of Engineering, University of Nottingham, Nottingham, UK.
[2] Instituto de Hidráulica Ambiental (IH), Universidad de Cantabria, E.T.S. Ingenieros de Caminos, C. y P., Av. de los Castros, s/n. 39005 Santander, Spain. E-mail: roland.garnier@unican.es
[3] Centro Andaluz de Medio Ambiente, Universidad de Granada, Granada, Spain.
[4] Departament de Física Aplicada, Universitat Politècnica de Catalunya, Campus Nord - Mòdul B4, 08034 Barcelona, Spain.

SUMMARY: Large beach cusps (LBC, wavelength of ~ 30 m) are intertidal features that can alternately exist in the swash and in the inner surf zone due to tidal sea level changes. They have a larger cross-shore extent (up to 50 m) than traditional cusps. This extent has been explained by a shift of the swash zone during falling tide. The cusps immerse at rising tide and previous studies indicate that surf zone processes are exclusively destructive. Here, the behaviour of large beach cusps in the inner surf zone is investigated by using a 2DH morphological numerical model applied to Trafalgar Beach (Cádiz, Spain). The model results indicate that the inner surf zone processes do not always destroy the cusps but can in fact reinforce them by considering neither the swash processes nor the tidal changes. More generally, in conditions favouring the presence of the LBC the surf zone of a beach can be unstable, leading to the formation of transverse/oblique sand bars that can have characteristics similar to the LBC. Thus, in principle, the LBC could emerge not only due to swash zone morphodynamics but also due to surf zone morphodynamics or a combination of both.

Keywords: beach cusps, surf zone, sand bars, instability, beach morphology, beach features, rip currents, wave processes on beaches.

RESUMEN: Formas cuspidales de playas y procesos de la zona de rompientes interna: crecimiento o destrucción? Aplicación a la playa de Trafalgar (Cádiz, España). – Las formas cuspidales de grandes dimensiones (LBC, longitudes de onda ~30 m) constituyen un sistema morfológico rítmico a lo largo de la playa que tiene una parte que se encuentra alternativamente en la zona de swash (flujo/reflujo) y en la zona de rompientes interna debido a los cambios del nivel del mar. Tienen una distancia de penetración de hasta 50 m, superior por tanto a la de las cúspides ordinarias. Esta elongación parece debido a la traslación de la zona de swash durante la marea descendente. En marea ascendente estas estructuras están sumergidas y los estudios previos consideran que los procesos de la zona de rompientes las destruyen. En este trabajo se analiza el comportamiento de estas formas en la zona de rompientes de la playa de Trafalgar (Cádiz) usando un modelo numérico morfológico 2DH. Los resultados muestran que, sin considerar ni los procesos de swash ni el cambio de marea, los procesos de la zona de rompientes no necesariamente destruyen LBC, sino que pueden reforzarlas. De forma más general, en condiciones favorables a la presencia de LBC, se pueden formar barras de arena con características similares a LBC debido a procesos de auto-organización en la zona de rompientes.

Palabras clave: cúspides de playa, zona de rompientes, inestabilidad, morfología de playas, estructura de playas, corriente de retorno superficial, procesos del oleaje sobre las playas.

INTRODUCTION

Beach cusps are a longitudinal regular series of horns and embayments which characterize an undulating shoreline. They have been listed with a large range of length scales: their wavelength λ_c (alongshore spacing between two consecutive horns) can range from centimetres to hundreds of metres. This is strongly related to their time scale, which is from minutes to days, respectively, and also to the wave period of the forcing conditions. The mechanisms at the origin of their formation can also differ, and there is still a large uncertainty regarding this.

The largest cusps are also called 'megacusps', 'giant cusps' or 'surf zone cusps' (λ_c~100 m). They are due to surf zone processes and commonly correspond to the shore attachment of transverse/oblique bars. These bars and the associated rip current circulation are very often related to an off-shore crescentic bar system (Inman and Guza, 1982; Wright and Short, 1984; Short, 1999; Ortega-Sánchez *et al.*, 2003; Calvete *et al.*, 2005; Castelle *et al.*, 2007; Garnier *et al.*, 2008).

The smaller cusps (λ_c~1-50 m) are considered standard beach cusps and are supposed to form by swash zone processes ('swash cusps'). Currently, two different main theories explain their formation (Masselink *et al.*, 1997; Coco *et al.*, 1999; Almar *et al.*, 2008): (1) the standing sub-harmonic edge wave theory (Guza and Inman, 1975; Holland and Holman, 1996) and (2) the self-organization theory (Werner and Fink, 1993; Masselink and Pattiaratchi, 1998; Coco *et al.*, 2000, 2003, 2004; Dodd *et al.*, 2008). The edge wave hypothesis can sometimes explain the initial formation of cusps for non-breaking waves, but not the further step of their evolution. Indeed, the presence of finite amplitude cusps theoretically inhibits the edge waves (Guza and Bowen, 1975), and some experimental studies show that cusps can exist in the absence of edge waves (Masselink *et al.*, 2004). Moreover, although Ciriano *et al.* (2005) observed the coexistence of cusps and edge waves, there was no evidence that edge waves were standing, which is a key requisite of the edge wave mechanism. In this theory the cusps grow as a reaction to a hydrodynamical instability. The self-organization theory is probably now the most accepted and can explain the entire evolution of the cusps in agreement with the observations, from their formation and their growth by positive feedback between flow and morphology until the saturation of their growth by diffusion processes. In a recent development in line with the self-organization approach, Dodd *et al.* (2008) showed that cusps can grow by an apparent hydrodynamical positive feedback mechanism that is intimately linked to bore driven swash, and is enhanced by morphological feedback.

The study of the rhythmic morphology at a sandy beach in Trafalgar (Spain) carried out by Ortega-Sánchez *et al.* (2008) distinguishes the smaller cusps (λ_c<20 m) from the 'large beach cusps' ('LBC', λ_c~30 m), based on the fact that the former have a shorter protruding distance S_c (cross-shore extent of a cusp) than the latter. The classification was made using the threshold value of S_c=5 m. The small cusps (S_c<5 m) appear in the upper beachface and are formed at high tide by swash processes. On the other hand, the large cusps (S_c>5 m) can have a protruding distance of up to S_c=50 m. This can be explained by the cross-shore shift of the swash zone due to the variation of the tide level (the tidal range is between 1.2 and 3.8 m at the study site).

Although the distinction between the small cusps, which are the most frequently observed, and the LBC had not been done before Ortega-Sánchez *et al.* (2008), other studies already reported the LBC in tidal environments (Holland, 1998; Coco *et al.*, 2004; Almar *et al.*, 2008). The LBC are distinguished from the small cusps as they do not appear exclusively on upper beach; they have a larger scale (wave length) and a larger protruding distance. Moreover the LBC are notable because they sometimes present an oblique orientation with respect to the mean shoreline, and they sometimes migrate alongshore. These distinctions suggest that different mechanisms could be at the origin of the formation of these cusps.

Coco *et al.* (2004) investigated the mechanisms behind the behaviour of cusps that are similar to the LBC observed at Trafalgar Beach. They find that the cusps grow during a falling tide because bays erode more than horns. They reproduce this behaviour as a result of self organization by using a numerical model based on the ballistic theory. Conversely their beach surveys indicate that the cusps wane during a rising tide. Two reasons are given. First, water particles infiltrate preferentially in embayments causing deposition. Second, the morphology is smoothed seaward of the swash front. They consider this effect, by including an extra diffusion term. Therefore, at the rising tide, when the previously formed cusps shift into the surf zone, they are damped. Their model results show that the main reason for the reduction of the cross-shore extent of cusps is the surf zone diffusivity rather than the swash processes.

However, surf zone modelling studies which do not consider the swash zone processes (Ribas *et al.*, 2003; Caballeria *et al.*, 2002; van Leeuwen *et al.*, 2006; Garnier *et al.*, 2006) show that not only can diffusion occur in the surf zone of a planar beach, but also instabilities can emerge from self-organization. In particular, the nonlinear 2DH study by Garnier *et al.* (2006) reveals the emergence of transverse bars with similar characteristics to the large cusps at Trafalgar Beach. These bars are found to be an equilibrium state of the surf zone. One limitation of these surf zone models is the assumption of a rectilinear absorbing wall at the shoreline boundary. Thus, the horizontal shoreline evolution is not taken into account. However, the bed level at the wall is allowed to move vertically and we can

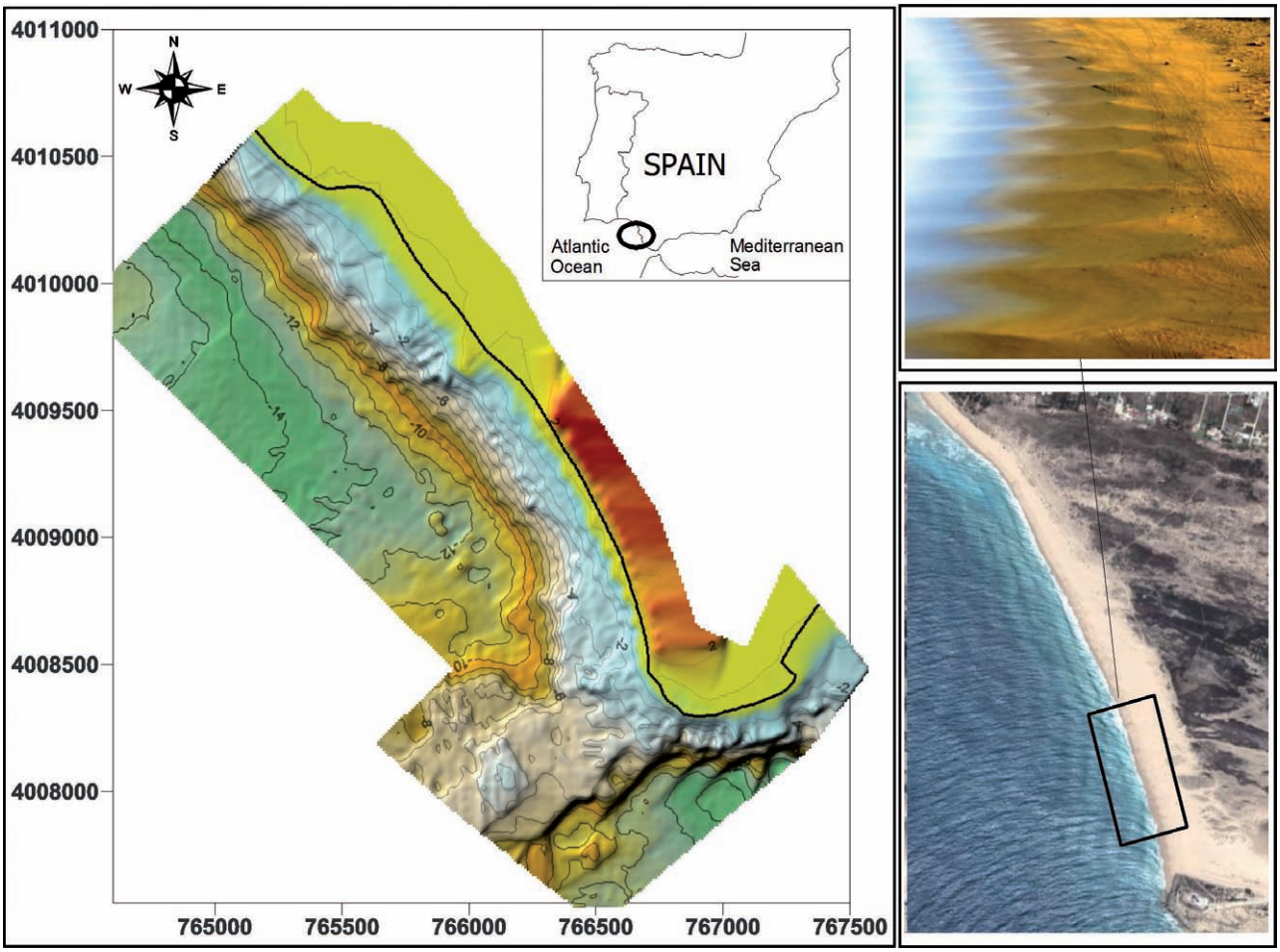

FIG. 1. – Location of the study site and detailed nearshore bathymetry of Trafalgar Beach surveyed in June 2006, with zoom on beach cusps.

consider that a horizontal oscillation of the shoreline is induced by the deposition/erosion of sediment next to the wall generating a horn/embayment at the shoreline, respectively. This assumption has been considered to explain the formation of megacusps (Calvete *et al.*, 2005; Garnier *et al.*, 2008), which are well known surf zone features.

Although Coco *et al.* (2004) succeeded in reproducing the general behaviour of the large cusps, and therefore the fact that they were damped in the surf zone, a specific surf zone instability study of a cuspate beach deserves attention. Furthermore, some cusp characteristics, such as the oblique orientation and the alongshore migration, were not correctly reproduced with their model. Thus, the main goal of this work is to study the morphodynamic instability of the surf zone of Trafalgar Beach for wave conditions and initial topographies typically measured during the large cusp events but in highly idealized conditions so as to focus on the basic 2DH processes. For instance, the swash zone processes are excluded and the tide level variations are not taken into account. This work will give insight into the possible growth of the LBC in the surf zone as an analogy with the megacusps. It will allow us to identify the morphological and hydrodynamical beach configuration that is favourable for this growth. Actually, a new and more general objective is here pursued: understanding the interaction between the swash and the surf zones through beach cusp behaviour.

The article is organized as follows. First, the study site and the data used are presented. Then, the rhythmic morphologies and some beach cusps formation events are selected and described. After that, the numerical model and the results are described. Finally, a conclusion is given.

STUDY SITE

Trafalgar Beach is located in a mesotidal and swell-dominated coastal environment along the southwest Spanish coast, in the Gulf of Cádiz (Fig. 1). It is an approximately 2-km-long sandy beach with a mean NNW-SSE alignment. The astronomical tide is semidiurnal, with an average amplitude of 2 m and a tidal range between 0.9 m and 4 m. Waves are predominantly from the west and break on the beach within a narrow breaking zone. A more complete description of the site is given by Ortega-Sánchez *et al.* (2008). For the

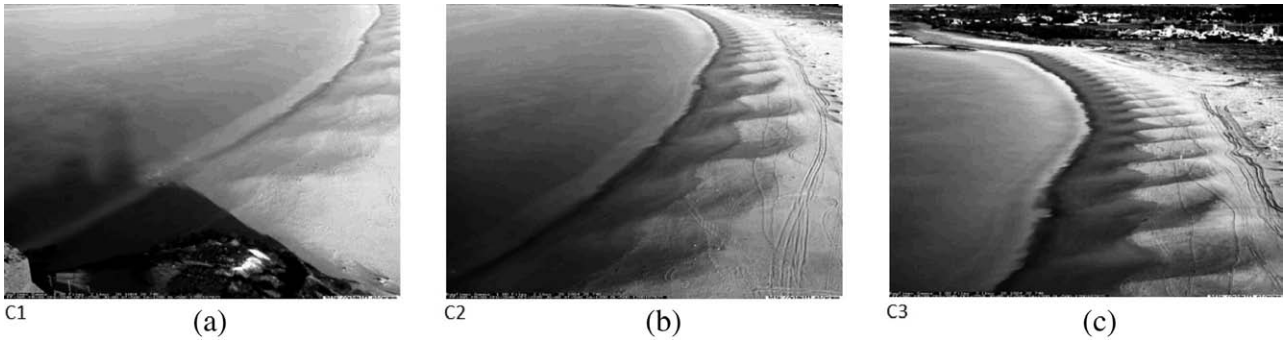

FIG. 2. – Examples of timex images from (a) camera 1 showing the part of the beach closest to Trafalgar Cape; (b) camera 2 looking to the middle of the beach, and (c) camera 3 visualizing the northern part of the beach. 26 January 2005.

predominant significant wave height, H_S=0.75 m, and the mean tidal range, T_R=2 m, the relative tidal range is 2.7. Estimating the settling velocity for a medium grain size of d_{50}=0.5 mm, and for a mean wave period of T=9 s, the beach-type parameter is Ω=1.2 (Wright and Short, 1984). This value is representative of a reflective beach, characterized by low-energy and long-period (swell) waves (Masselink and Short, 1993).

Nearshore bathymetry and beach topography measured in 2006 showed that Trafalgar Beach has a width of 40-70 m, increasing towards Trafalgar Cape. It is composed of medium and coarse sand ranging from 0.35 to 1 mm. A plane beach morphology dominates the nearshore zone and no alongshore sand bars were found (Fig. 1). The beach frequently exhibits rhythmic features of different dimensions, with beach cusps being the most common ones (Fig. 1). It can also frequently be observed that the geometrical characteristics of the cusps vary alongshore, being different close to the cape and far from it. The average beach slope within the cuspate features ranges between 0.06 and 0.10 for the cusp embayments and between 0.10 and 0.18 for the cusp horns. The nearshore beach slope away from the cuspate features ranges between 0.016 near the Cape and 0.026 close to the northern end of the study area.

DATA

Video images

In October 2003 a video-monitoring station based on the ARGUS technique (Aarninkhof and Holman, 1999; Holman and Stanley, 2007) was installed at the Trafalgar lighthouse, 50 m above mean sea level. The station includes 3 video cameras that collect an instantaneous image (snapshot), a 10-minute time-averaged image (timex) and a variance image every 10 minutes. Hourly images from each day were themselves averaged to create a 'daytimex', a composite image that reveals the daily mean morphology (Fig. 2).

Using the technique presented by Holland *et al.* (1997), video images are georeferenced and morphological features can be digitized to estimate their geometrical characteristics. The accuracy of this process is typically one pixel. In the present paper we will concentrate on midbeach, so one pixel corresponds to a ground accuracy of 0.25 and 1.4 m in the cross-shore and alongshore directions, respectively.

Large beach cusps: general description

Geometrical characteristics

Ortega-Sánchez *et al.* (2008) analysed 2 years of daily time exposure video images from the Argus station to explore the variability of the beachface morphology. Five different morphological states related to the presence or absence of beach cusps and a berm were found: (1) large beach cusps, (2) short-protruding beach cusps, (3) low tide terraces, (4) plane beach berms and (5) plane beaches. The main 'characteristic' morphological feature of the large

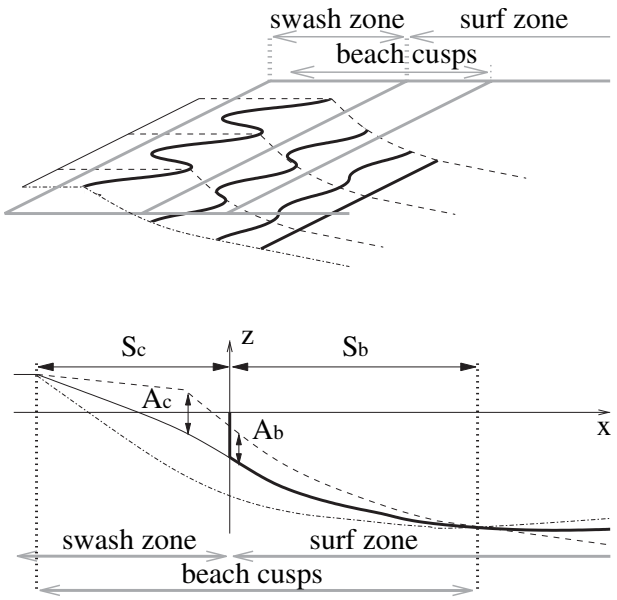

FIG. 3. – Main beach cusp characteristics for a fixed tide. S_c and A_c are the protruding distance and the amplitude of the part of the cusps that is in the swash zone, i.e. these parameters are measured at Trafalgar Beach. S_b and A_b correspond to the surf zone part of the cusps, i.e., where cusps can be interpreted as bars (they are model results). Notice that S_c and A_c are measured at low tide, and S_b and A_b change with the tide level.

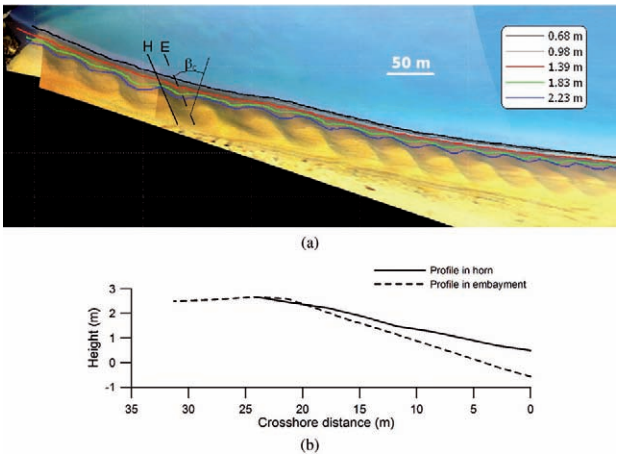

FIG. 4. – (a) Plan view of the beach showing LBC morphology, 26 January 2005. (b) Cross-shore profiles, 8 May 2006.

beach cusps is the protruding distance S_c (Fig. 3). It is defined as the cross-shore span of a horn, so that, if the angle between the cusp horn and the coastline normal is β_c, the 2D (horizontal) extent of a cusp is $S_c/\cos(\beta_c)$ (Fig. 4). S_c is always larger than 5 m, with some measurements showing values up to 50 m. Large beach cusps (LBC) correspond to the predominant beachface morphology and are present 60% of the time. LBC are located across the intertidal zone and during high tide waves can break within the embayments. Thus, cusps seem to be interacting with both surf and swash processes. Several of their characteristics are reminiscent of surf zone rhythmic features that appear by self-organization (Ribas *et al.*, 2003; Garnier *et al.*, 2006). The first of these are their length scale, i.e. their protruding distance, their wavelength λ_c (or spacing) and their amplitude

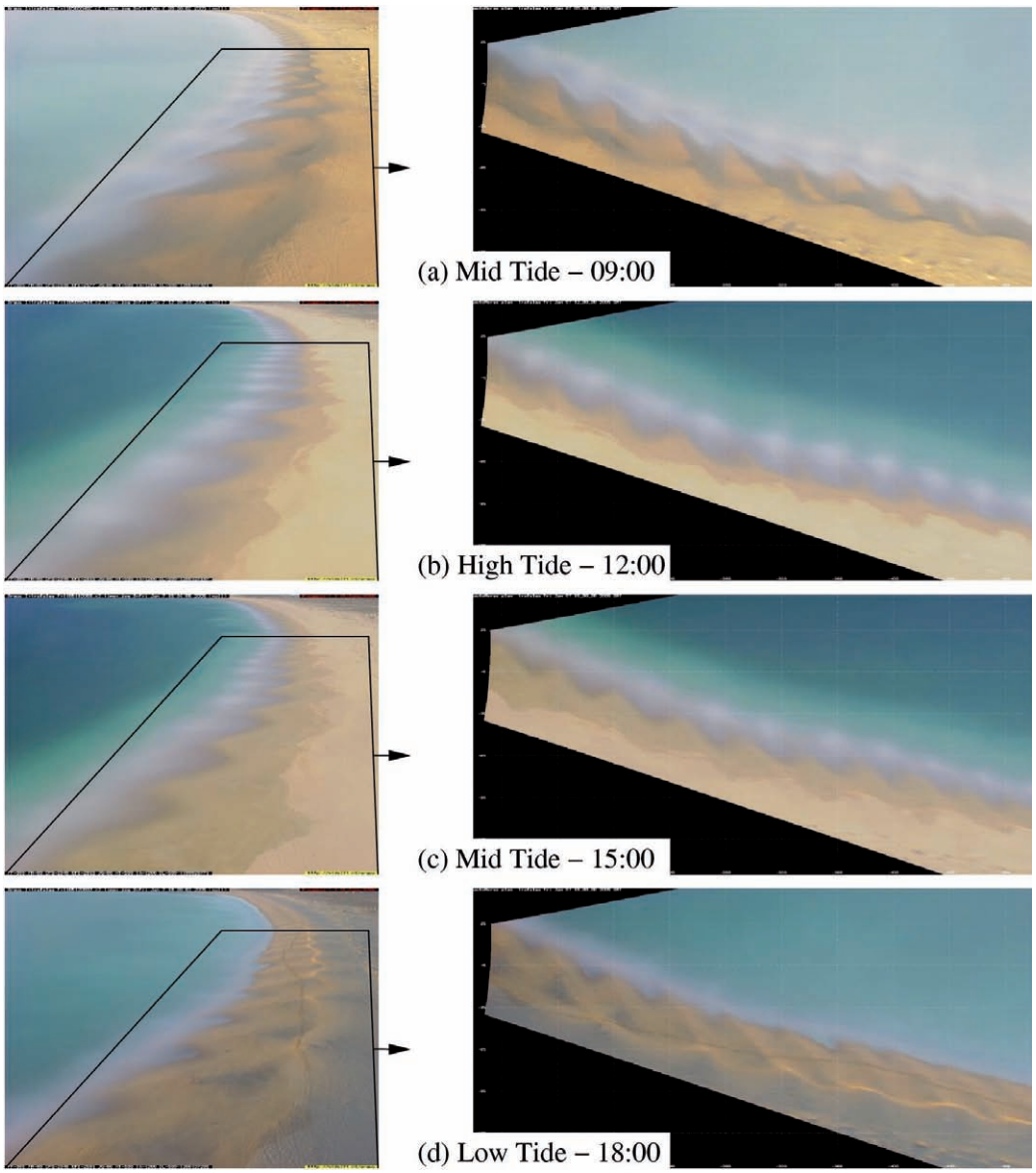

FIG. 5. – Snapshot of the cusps during a tide excursion, 7 January 2005. Left: timex images from camera 2. Right: Plan view after rectification.

A_c . Their mean spacing is 30 m but this can vary alongshore, being larger closer to the Cape (around 35 m) than in the north (20 m). A spacing of up to 60 m is sometimes observed. We define the amplitude A_c of a cusp as half the height between two consecutive horns and embayments (Fig. 3). As stated above, large cusps are located across the intertidal zone. Thus, the cusp amplitude can frequently reach values of up to 0.8 m. For instance, Figure 4b shows the cross-shore profile measured with a DGPS of a cusp with an amplitude of 0.5 m. The second similarity is that they are frequently oblique with respect to the initially straight shoreline (Fig. 4a). Notice that Figures 4a and 4b do not correspond to the same day, due to the poor quality of the plan-view images during the DGPS measurements.

The procedure for rectifying the video images is based on the assumption of a particular vertical elevation for all pixels of an image (Holland *et al.*, 1997; Holman and Stanley, 2007). When one is studying the sea surface this can be a reasonable assumption, but when one is studying morphological features of the beachface it can lead to additional errors, especially when the tidal range is important. If the upper part of the beach is 1 m above projection level (mean sea water level) it will be misplaced in the horizontal by a distance R/z_c, where R is the range from the camera (around 200 m in the present study) and z_c is the height of the camera above mean sea water level (i.e. around 50 m at Trafalgar Beach). If the tidal range is T_R, the error in the horizontal distance can be up to $T_R R/z_c$, so the error in the observed cusp angle can be estimated. This error is lower if the rectification is performed under high tide and, fortunately, oblique LBC are also observed (Fig. 5) there. Moreover, sea surface transverse and oblique circulations are also frequently observed (Fig. 6) with angles of up to 50°, and this is a reliable value.

Therefore, their similitude to surf zone bars and their appearance in the surf zone are reasons for thinking that surf zone processes can contribute to the growth and evolution of large beach cusps.

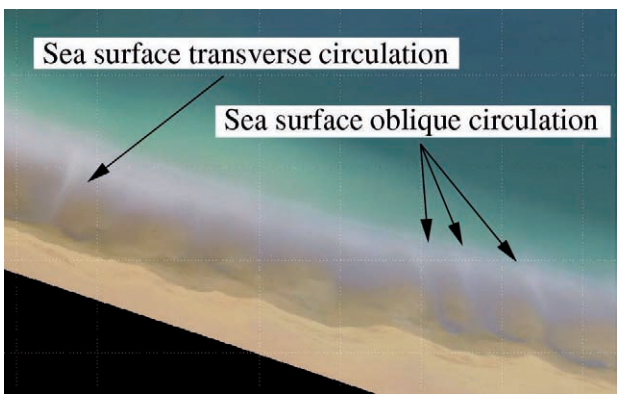

FIG. 6. – Sea-surface transverse and oblique circulations, 3 March 2004.

Favorable conditions

Large beach cusps are the main beachface morphology at Trafalgar Beach, and can be found 60% of the time (average). Although previous studies show that their large cross-shore extent is linked to the shift of the swash zone due to tide, there is no clear link between their protruding distance and the tidal range in Trafalgar. Moreover, the occurrence of the LBC is not clearly associated with spring tides. Actually their occurrence seems to be in strong relation to the wave conditions, even if the initial beach profile and the tidal range likely condition their emergence. Assuming an initial, plane beachface (e.g. after a storm), LBC are generally formed for offshore wave periods over T~7 s and offshore significant wave heights below H^{∞}_s~2.5 m, although they can be formed with higher waves (they were not found for offshore significant wave heights over 4 m). Their particular geometrical characteristics depend on the wave values. Thus, LBC are easily formed and predominate for low-to-medium wave energy conditions and medium-to-large wave periods. Ortega-Sánchez *et al.* (2008) found that the wave period was the main parameter controlling the transition from large beach cusps (large wave periods) to short-protruding beach cusps (short period waves). LBC can remain stable until the wave period forcing conditions change: if the wave period decreases (below T~7 s) and is maintained for enough time, the morphology will change to short-protruding beach cusps. This time depends on the energy content of the new forcing conditions, which explains why LBC are sometimes found under short wave periods. SWAN model propagation results indicated that, for the principal beach alignment, predominant offshore waves impinge on the beach within a range of obliquity of 0-20 degrees, with usual values of 5-15 degrees. These values do not affect the formation (or not) of the large beach cusps, whereas they seem to play an important role in their final geometrical characteristics.

Time scale

Determination of the exact time scale required for the formation of the different beachface morphologies found at Trafalgar Beach was difficult since frequently this included the night, when no images were available. However, an order of magnitude could be established that depends on the energy forcing conditions. For offshore significant wave heights over 2.5 m (high energy conditions), the large beach cusps were formed in a few hours (3-6 h), although these conditions are not frequently found. If the wave heights decrease to moderate energy conditions (between 1.5 and 2.5 m), almost half a day is required (9-12 h). Finally, for the predominant low energy conditions (offshore significant wave heights below 1.5 m) a few days are required (2-3 days). These times are also affected by the previous morphology (e.g. beachface slope). Once the LBC

TABLE 1. – Tidal range and initial wave conditions for the selected events of LBC formation (offshore waves: WANA; nearshore waves: SWAN).

Event	Date	Tidal range [m]	Averaged WANA data H^{∞}_{rms} [m]	T [s]	Direction [deg]	SWAN estimations (4 m depth) H^{0}_{rms} [m]	Direction [deg]	θ^{0}_{max} [deg]	θ^{0}_{min} [deg]	θ^{0} [deg]
Event 1	22-23 Dec. 2003	3.3	0.5 - 0.8	9-10	250	0.8-1.1	250	10	-15	-5
Event 2	28-29 Dec. 2003	2.2	1.1	12	290	1.1	270	30	-5	15
Event 3	20 Apr. 2004	2.4	0.8 - 1	11.5	285	0.8 - 1	265	25	0	10
Event 4	17 May 2004	2	1	14	290	1	270	30	-5	15
Event 5	23 Oct. 2004	1.8	1.2	10-11	275	1.2	260	20	-5	5
Event 6	01 Nov. 2004	1.7	1	9	270	1.2	260	20	-5	5
Event 7	26-27 Dec. 2004	2	0.7	11.2	290	0.7	270	30	-5	15

are formed, they remain until the forcing conditions are modified (see previous section).

Particular formation events

Two years of daily video images (2003-2005) were analysed to identify events when LBC were formed. A total of 15 events were identified, and 7 of them were selected to characterize the evolution of the morphology. Table 1 summarizes the initial hydrodynamical data, where WANA data corresponds to daily offshore wave forecast output in the area (Ortega-Sánchez *et al.*, 2008) provided by Puertos del Estado (Spain). These initial offshore wave data were propagated using the SWAN model (Booij *et al.*, 1999), and nearshore wave data were extracted at 4 m depth (Table 1). Wave heights vary slightly in the propagation, whereas wave angle decreases due to refraction. The last column of Table 1 shows the wave obliquity with respect to the mean alignment of the shoreline. The beach alignment is not completely straight, but slightly curved, the angle between the north and the shore normal varying from 240 to 265 degrees. Accordingly, three numbers are included for the wave angle at 4 m depth: (1) θ^{0}_{max} indicates the difference with respect to 240, (2) θ^{0}_{min} indicates the difference with respect to 265, and (3) θ^{0} indicates the relative orientation with respect to the beach alignment where the large beach cusps are best formed (255 degrees) and is considered as the most realistic.

Table 2 summarizes the main geometrical and evolutionary characteristics of the morphologies of the events, including the cusp spacing or wavelength, the obliquity or orientation, the protruding distance and the amplitude. The variability of the spacing for the same event is due to the longshore variability of the morphology (Ortega-Sánchez *et al.*, 2008). According to the wave data, oblique large beach cusps are formed under low wave-energy conditions (H_s<1.2 m), with peak periods varying within 9-14 s that impinge obliquely to the coast (similar results were found by Ortega-Sánchez *et al.* (2008)).

The cusp wave length varies from 25 to 40 m (approximately), the predominant value being around 30-35 m. Events 1 and 6 show the minor spacing, which seems to be associated with the lower period (9 s), whereas the higher wavelengths are found for the higher periods (12 s).

TABLE 2. – Cusp characteristics after complete formation of the events: wave length λ_c, orientation β_c, protruding distance S_c and amplitude A_c. An indicative maximum error is given for the cusp angle β_c, by assuming that it has been measured at low tide, and that the error in the horizontal displacement is $T_R R/z_c$

Event	λ_c [m]	β_c [deg]	S_c [m]	A_c [m]
Event 1	26-27	38±25	24	0.8
Event 2	35	50±8	29	0.6
Event 3	35-40	12±13	40	0.6
Event 4	33	49±6	37	0.5
Event 5	32-39	37±6	45	0.38
Event 6	28-30	38±6	40	0.43
Event 7	30-33	26±12	33	0.48

Cusp orientation varies within 25-50 degrees. Events 2 and 4 correspond to very oblique incoming waves, showing very oblique cusps; event 7, although showing the same incoming wave direction, does not show the same obliquity, seemingly due to very low energy waves. The rest of the orientations are, in general, around 35 degrees. The orientation in event 3 would be expected to be higher, but on the previous days there were higher waves (almost 3 m) that must play an important role in that difference.

MODELLING

The MORFO55 numerical model has been used to analyse the morphodynamical instability of the surf zone of Trafalgar Beach. MORFO55 is a 2DH morphodynamical model based on a wave- and depth-averaged nonlinear shallow water equations solver with wave driver, sediment transport and bed updating (Garnier *et al.*, 2006). It is able to reproduce the formation and the long-term evolution of rhythmic sand bars as free instabilities of alongshore uniform beaches excited by a small perturbation added on the initial topography (Garnier *et al.*, 2006, 2008). In particular, Garnier *et al.* (2006) show that small-scale transverse/oblique bars (λ_b~30 m) can develop on planar beaches from self-organization mechanisms. However, their emergence strongly depends on the sediment transport parameterization and its formulation has a large degree of uncertainty. The general formulation chosen is based on the total load formula of Soulsby and Van Rijn (Soulsby, 1997). The horizontal sediment flux vector reads:

$$\vec{q} = a\left(\vec{v} - \gamma u_b \vec{\nabla} h\right) \quad (1)$$

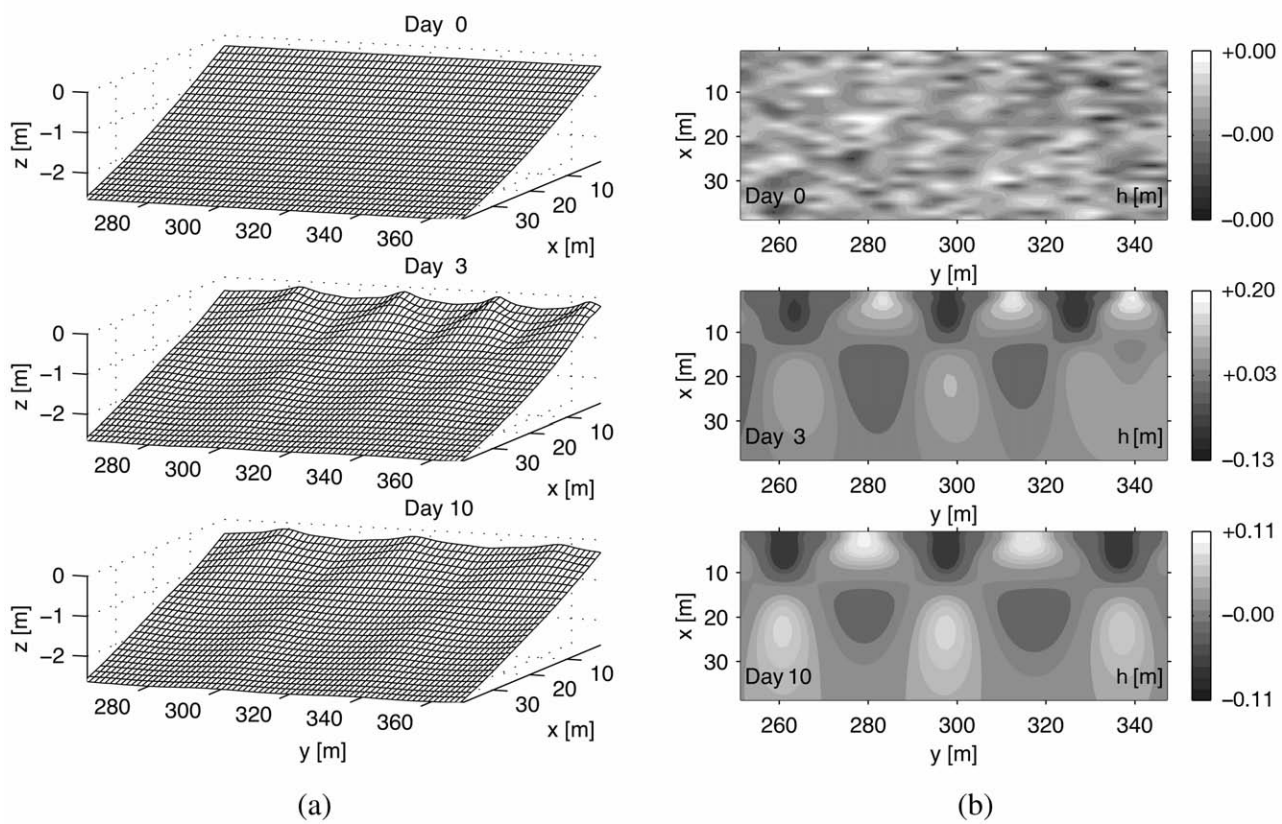

FIG. 7. – Default case. Snapshots of (a) a part of the topography (three-dimensional view) and (b) the bed level perturbation h in m (top view). From top to bottom: Day 0, Day 3 and Day 10.

where α is the stirring factor, γ is the bedslope coefficient, u_b is the root-mean-square wave orbital velocity amplitude at the bottom and h is the bed-level deviation from the initial alongshore uniform topography.

Two different stirring factors are tested here, a constant wave stirring (CWS) ($\alpha=\alpha_0=0.01$ m) and the formula of Soulsby and Van Rijn (SVR) ($\alpha=\alpha_{SVR}$). The latter depends essentially on sediment characteristics, water depth, wave orbital velocity and current. Despite the numerous existing sediment transport formulations, the modelling studies by Ribas *et al.* (2003) and Garnier *et al.* (2006) show that the use of these two particular formulae allows us to consider all the possible physical configurations of morphological instabilities that can be obtained with our model. The emergence of the instability is strongly related to the depth averaged sediment concentration (also called potential stirring) which is defined as $C=\alpha/D$, where D is the total depth (Falqués *et al.*, 2000); in particular, for $\alpha=\alpha_0$, the averaged cross-shore profile of C decreases off-shore, while for $\alpha=\alpha_{SVR}$ it increases offshore up to a certain point and eventually decreases. Garnier *et al.* (2006) found that a planar beach can be unstable for $\alpha=\alpha_{SVR}$, whatever the incidence wave angle, while the use of $\alpha=\alpha_0$ requires $\theta^0>20°$ to observe instability (in their particular experiment, i.e. θ^0 was defined at 3 m depth).

The use of α_0 is less physically founded than the SVR formula, but it is a possible method by which a higher proportion of infra-gravity waves can be included. Moreover, recent experiments reveal that breaking generated turbulence and wave bores entrain a higher concentration in the inner surf zone (Johnson and Smith, 2008), which is not represented by the traditional transport formulae such as the SVR formula, in which the concentration profile is mainly controlled by the wave orbital velocity, and which decays onshore from the breaking point. To be consistent with the SVR formula, the value of α_0 has been set to the maximum value of α_{SVR} ($\alpha_0=0.01$ m for the default case).

The beach profile used for the experiments is exponential, with an off-shore slope of 0.02 and a shoreline slope of β_0. An artificial absorbing wall is imposed at the shoreline with height of α_0. The offshore boundary is located at $x=L_x=85$ m, where the depth is approximately 4 m. At the offshore boundary, constant waves are imposed with the root mean square height H^0_{rms}, period T and angle θ^0 ($\theta^0=0$ corresponds to normal wave incidence). The sediment size is defined through the parameter d_{50}.

The initial topography consists of an alongshore uniform beach where a perturbation h(x,y,t=0) can be added to excite the instabilities, or to simulate the evolution of pre-existing rhythmic features. The alongshore size of the domain is defined as $L_y=300$ m. The

cross-shore and alongshore grid spacing are 1.5 m. The morphodynamic time step is 1.14 s.

The first part of the modelling study is dedicated to understanding the formation of cusps as a free instability of the beach, by adding a small random perturbation to the bathymetry. The default case was chosen as the most characteristic large cusps event, except that normal waves are assumed. A parametric study was made, varying the sediment transport, the wave conditions, and the beach properties, consistent with the observations. The second part consists of simulating the behaviour of pre-existing cusps to test their decay or maintenance. First, we impose different initial wavelengths for the three model settings leading to different kinds of instabilities and, second, we investigate the damping of pre-existing cusps (for a fixed wavelength) for the parameters leading to stability.

Free instability

At the initial time, small random perturbations are imposed on the alongshore uniform topography in order to excite the beach system and leave the instability free to develop. The default initial topography is displayed in Figure 7a (Day 0), the maximum bed level perturbation amplitude being 1 mm.

Default case

For the default case, waves are assumed to arrive normally to the coast (θ^0=0°) and the wave height and period are set to H^0_{rms}=1 m, T=9 s. The SVR transport is used. The slope at the shoreline is the mean slope found in an embayment: β_0=0.075. The height of the shoreline wall is a_0=20 cm. The sediment size is d_{50}=0.5 mm.

This case is unstable and a transverse bar system develops with a growth rate of σ_b=5 day^{-1} (Fig. 8). From the Fourier analysis of the longshore section x=5 m (Fig. 8b), the growth rate can be computed for the full range of wavelengths (for $0<\lambda_b<L_y$). For each time step, we only retain the growth rate corresponding to the wavelength, which is predominant and which is physical (Figs. 8d-f), i.e. these wavelengths vary in time from λ_b=26 m to λ_b=37 m and stabilize at the equilibrium state at λ_b=35 m. We remark that the growth rate computed for each of these wavelengths is similar during the initial development of the instabilities.

Instability modes

From all the experiments, we distinguish three kinds of instabilities, also called instability modes. They are: (1) transverse bars as in the default case, which occur for normal waves; (2) oblique down-current oriented bars, occurring for oblique wave incidence and by computing the stirring factor with the Soulsby and Van Rijn formula $\alpha=\alpha_{SVR}$; and (3) Oblique up-current oriented bars, occurring for oblique wave incidence with a constant wave stirring ($\alpha=\alpha_0$). Figure 9 displays an example of these three modes, for wave height H^0_{rms}=1 m and wave period T=9 s, and for the other settings of the default case (the default case is shown in Fig. 9a), except for the wave angle fixed to θ^0=10° in Figures 9b and 9c, and for the sediment transport where $\alpha=\alpha_0$ in Figures 9c.

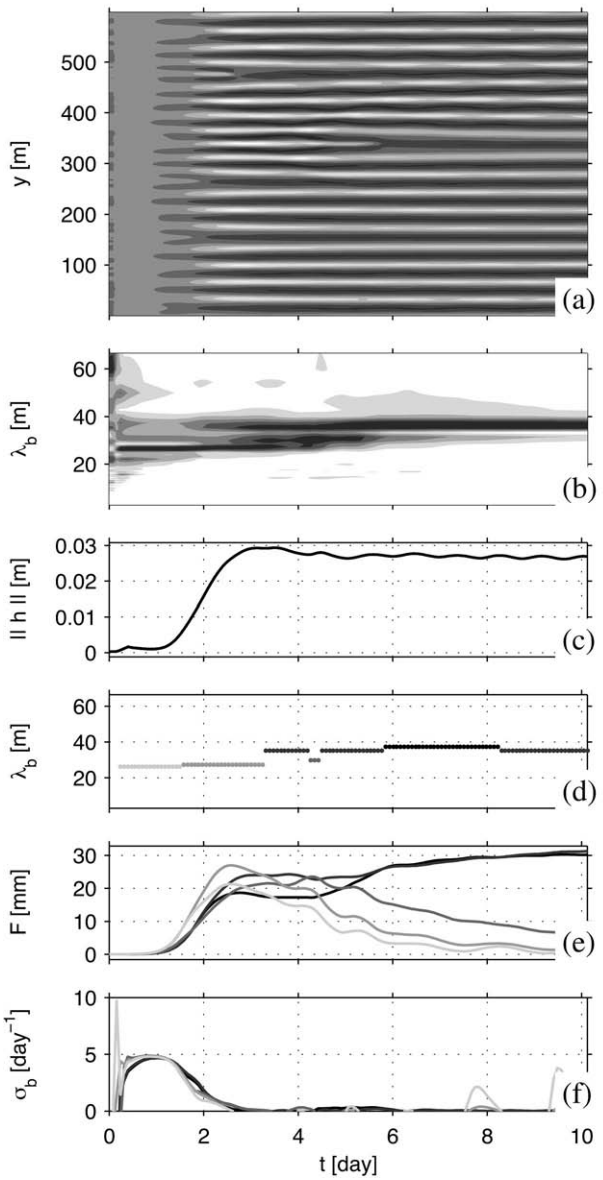

FIG. 8. – Time series of (a) the bed level perturbation h along a longshore section, (b) its Fourier analysis, (c) the bar norm |h|, (d) the dominant wavelength λ_b, (e) the Fourier coefficient of the corresponding modes and (f) the growth rate of the corresponding modes σ_b.

TABLE 3. – Instability modes: wave length λ_b, growth rate σ_b, wave length at the equilibrium state λ_{be}, orientation β_b, protruding distance S_b and amplitude A_b.

Mode	λ_b [m]	σ_b [/day]	λ_{be} [m]	β_b [deg]	S_b [m]	A_b [m]
(1)	26-37	4.8	35	0	10	0.13
(2)	19-33	1.4	31	53	43	0.21
(3)	50-100	1.9	100	-53	67	0.5

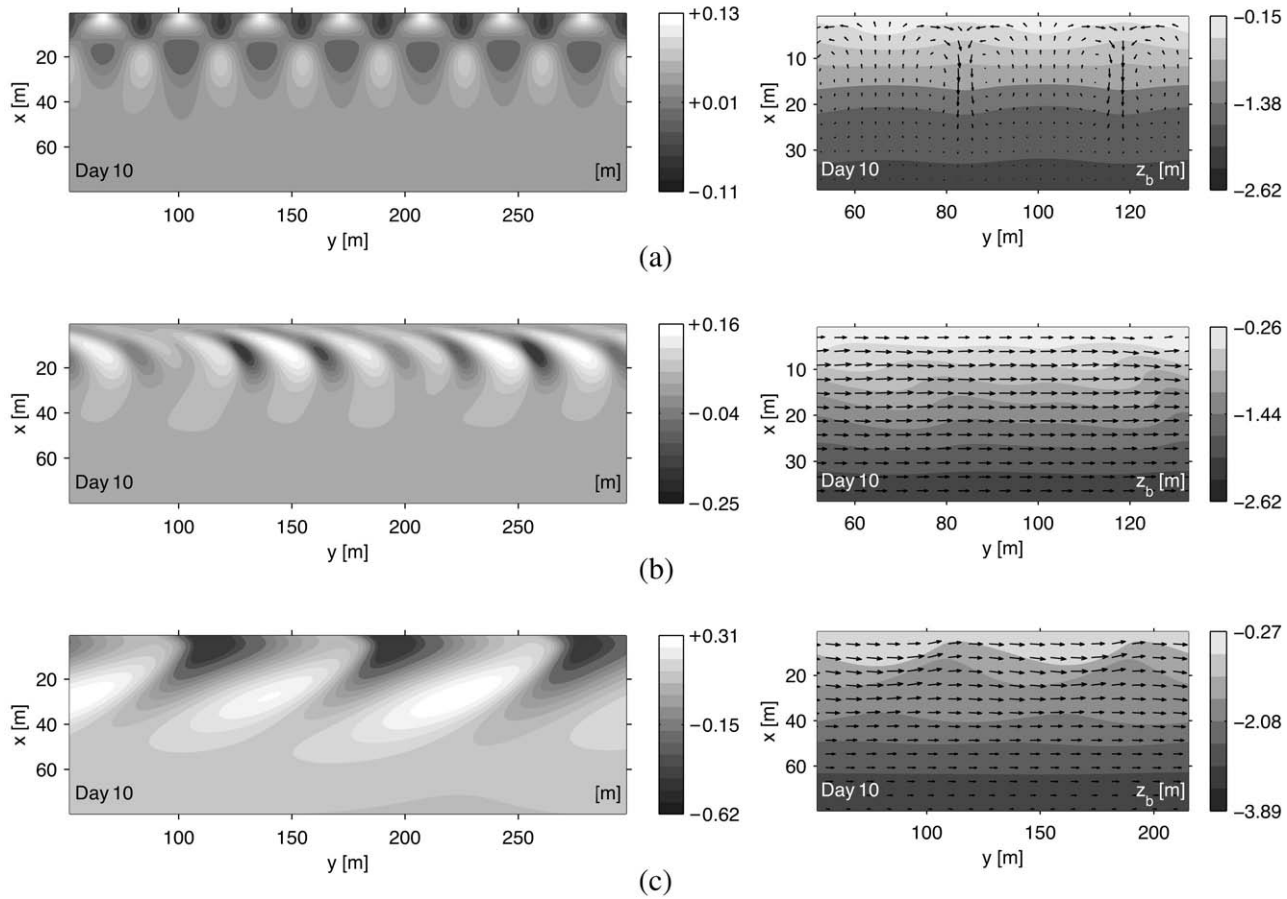

FIG. 9. – Final states (Day 10) of the different kinds of instabilities obtained for H^0_{rms}=1 m and T=9 s. Left: bed level perturbation h. Right: bed level z_b and current vectors. (a) Transverse bars (SVR sediment transport, θ^0=0), maximum current 0.5 ms^{-1}. (b) Down-current oblique bars (SVR sediment transport, θ^0=10°), maximum current 1.4 ms^{-1}. (c) Up-current oblique bars (CWS sediment transport, θ^0=10°), maximum current 1.2 ms^{-1}.

The main characteristics of the bars are shown in Table 3. The bar orientation β_b, the protruding distance S_b and the amplitude A_b are measured at the equilibrium state. S_b is defined as the mean cross-shore extent of the bars from x=0 m to the location where their amplitude is 5% of A_b. A_b is computed as A_b=0.5(max(h)-min(h)). Finally, the bar orientation is subjective as the angle changes with the cross-shore location. Here, the bar angle was computed at the cross-shore position where h is maximum. The down-current bar angle is higher at the shoreline and decreases off-shore. It becomes negative at the bar tip. The obliquity of up-current bars is larger off-shore.

The length scale of the transverse bars and of the oblique down-current bars are similar. Although the oblique bars are smaller in wave length, they have a larger protruding distance. Actually, the cross-shore extension of the bedforms is the same if we include the anti-phase system off-shore of the transverse bars: to be precise, each bar (channel) is extended off-shore by a channel (bar) with smaller amplitude. The length scale of up-current bars is larger than the other modes. The time scale of the transverse bars is shorter (larger growth rate) than that of the oblique bars.

Table 4. – Parametric trends: wave length λ_b, growth rate σ_b, wave length at the equilibrium state λ_{be}, orientation β_b, protruding distance S_b and amplitude A_b. No value has been displayed in the λ_{be} column when overflow occurred in one of the experiments. The left column indicates the input parameters that have been changed with respect to the default case, i.e., with respect to θ^0=0, H^0_{rms}=1 m, T=9 s, β_0=0.075, d_{50}=0.5 mm and $\alpha=\alpha_{SVR}$.

Parameter	λ_b [m]	σ_b [/day]	λ_{be} [m]	β_b [deg]	S_b [m]	A_b [m]
θ^0=1°-15°	19-37	0.0-1.5	–	45-63	31-43	0.00-0.65
H^0_{rms}=0.7-1.2 m	26-40	4.5-4.8	27-40	0	8-13	0.08-0.16
T=9–14 s	27-37	4.8-5.1	33-35	0	10	0.08-0.13
β_0=0.05-0.15	26-37	0.0-5.5	–	0	7-20	0.00-0.45
d_{50}=0.25-1.00 mm	26-37	4.1-6.6	–	0	10-12	0.13-0.35
$\alpha=\alpha_0$, θ^0=1°-15°	46-120	0.0-2.2	46-120	–45- –67	67-70	0.00-0.50

Varying the wave conditions

Table 4 summarizes the bar properties by varying the model parameters. As suggested in the previous section, the kind of instability obtained strongly depends on the incident wave angle. Here, the range of incident wave angle (at 4 m depth) found during the Trafalgar cusp events was tested ($0<\theta^0\leq 15°$). As soon as a weak obliquity is imposed (even for $\theta^0=1°$), the instability mode differs and the transverse bars do not emerge. For $0<\theta^0\leq 2°$ and $\theta^0>10°$, the beach system is stable. For $2°<\theta^0\leq 10°$ oblique down-current bars appear. In some experiments, the model overflows, so equilibrium is not reached. However, the growth rate and the wavelength of the emerging instability can be computed. The growth rate is always smaller than that obtained for normal wave incidence, but the wavelength of the bar is similar, so similar to the cusp wavelength observed in Trafalgar. The sensitivity of the model to the imposed incident wave angle (i.e. different modes for $\theta^0=0$, 1° and 2°) is not comparable with observations as it corresponds to the uncertainty in wave angle measurements. Furthermore, the wave angle is never regular in nature. However, the present results show the possibility of the emergence of two kinds of instability for normal or near-normal wave incidence, which are comparable, in length scale, to the Trafalgar cusps. Moreover, for strong obliquity ($\theta^0>10°$), we obtain stability.

For the wave heights and the wave periods observed at Trafalgar Beach during the cusp events (i.e. $9\leq T\leq 14$ s and $0.7\leq H^0_{rms}\leq 1.2$ m), the surf zone is unstable, and the growth rates are similar (i.e. to the default case). The largest variation in bar properties occurs in the wavelength when the wave height varies, i.e. $27\leq \lambda_{be}\leq 40$ m: the higher the wave, the larger the wavelength.

The presented cusp formation events have an offshore wave height of less than 1.2 m (H^∞_{rms} Table 1), which corresponds to $H^0_{rms}=1.2$ m at 4 m depth. Higher wave conditions are not representative of the large cusp events observed at Trafalgar Beach. However, LBC can be observed for high energetic waves, with heights of up to $H^\infty_{rms}\approx 1.8$ m. This is in agreement with the model results, as these big waves dissipate at a depth greater than 4 m and correspond, at 4 m depth, to waves of $H^0_{rms}\approx 1.2$ m. Thus, the model predicts instability for these waves.

For higher waves, $H^\infty_{rms}>2$ m, the LBC are generally destroyed at Trafalgar Beach. These wave conditions cannot be simulated as the model neglects the cross-shore surf-zone processes that are essential for high-energy wave conditions.

Varying the beach characteristics

Even in the absence of beach cusps, the beach slope of Trafalgar Beach may vary alongshore. Moreover, due to the large beach cusps, the slope at the shoreline differs if we consider a horn or a bay. In our experiments, the beach profile is assumed to be alongshore-uniform and the beach slope at the shore boundary β_0 (at 20 cm depth) and at the off-shore boundary (at 3 m depth) is constant. While the instability of the beach is not sensitive to the off-shore beach slope, β_0 can affect the results. A large range has been tested by varying β_0 as $0.05<\beta_0<0.15$ (Table 4). When β_0 decreases, the surf zone width increases and the bedforms are therefore larger (we observe the same wavelength, but A_b and S_b are larger). For the largest beach slope, $\beta_0=0.15$, the depth at the shoreline seems too deep to allow the (smallest) bedforms to develop, and the beach is found to be stable.

Because of the inhomogeneity in sand size at Trafalgar Beach, we tested different sediment sizes ($0.25<d_{50}<1$ mm). The growth rate decreases when the sediment size is set larger; however, even for the largest sediment size present at Trafalgar Beach ($d_{50}=1$ mm), the surf zone is still found to be unstable.

CWS sediment transport

The use of a constant wave stirring ($\alpha=\alpha_0$) leads to the emergence of up-current bars only in the presence of a longshore current. The previous study by Garnier *et al.* (2006) shows that the up-current bars grow faster if the off-shore wave angle is larger. Table 4 shows the bar characteristics if the wave angle is changed from $1°\leq \theta^0\leq 15°$. For $\theta^0<3°$, the beach is stable, and the growth rate increases with an increasing obliquity. Moreover, for larger θ^0, the size of the bars (λ_{be}, S_b and A_b) and their obliquity become larger.

As discussed by Garnier *et al.* (2006), the uncertainty in sediment transport formulae and the lack of measurements of averaged sediment concentration in the surf zone explain our desire to study these two formulae; they are fundamentally different, as α_{SVR} gives a peak in the potential stirring (i.e. depth-averaged concentration $C=\alpha/S$) cross-shore profile, while α_0 gives an offshore decreasing C. Interestingly, whatever the incident wave angle, instability can be observed for some stirring factor: for small wave angles α_{SVR} gives instability, while large angle instability is obtained for α_0. Only for a small range of wave angles do both formulae give instability: here, it occurs for $3°<\theta^0<8°$ (at 4 m depth), but this range corresponds to the main wave angle observed at Trafalgar Beach. Conclusions on the validity of the two formulae are difficult to give with the Argus system, unless it is used with instruments deployed in the surf zone to measure the sediment concentration.

The present study is a first step towards understanding the processes behind the surf zone instability that can occur at Trafalgar Beach. A more realistic comparison would need sediment concentration measurements, in addition to the consideration of a real irregular wave forcing and a real initial topography that is not rectilinear, showing a difference in wave angle at 4 m of up to ±20° depending on the alongshore location (Table 1).

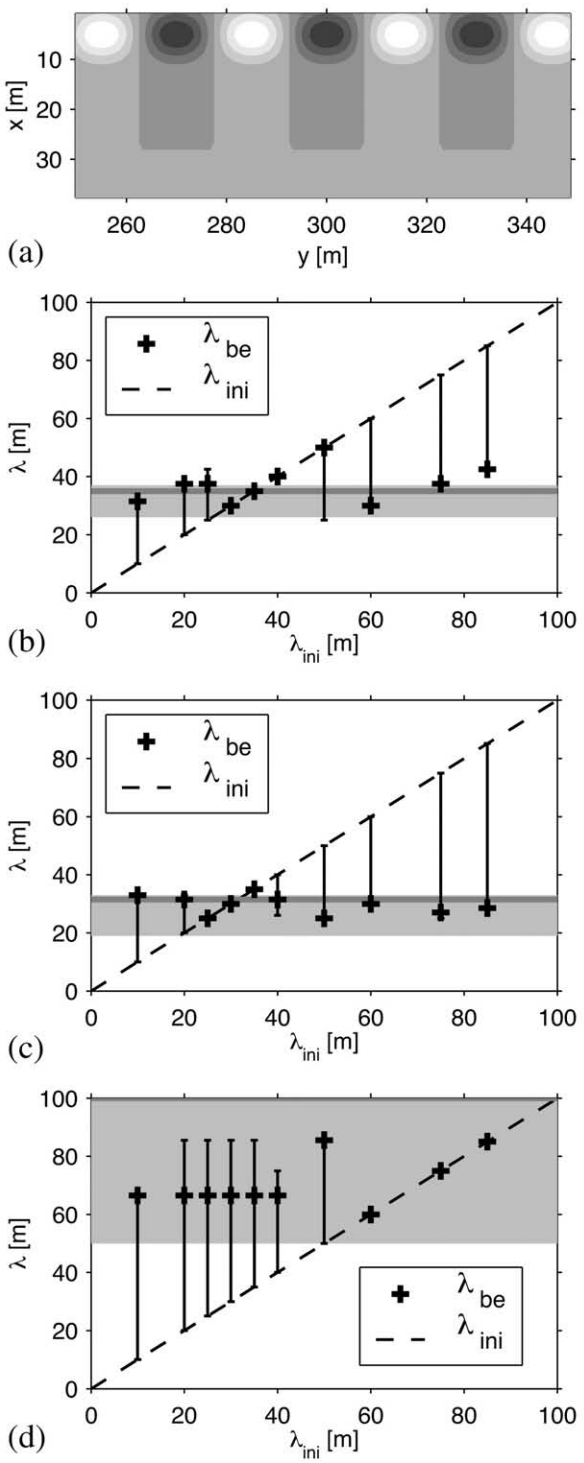

FIG. 10. – (a) Initial bed level perturbation (h), for λ_{ini}=30 m. (b-d) Influence of the preexisting cusp wavelength on the final wavelength. (b) Transverse bars (SVR sediment transport, θ^0=0), (c) Down-current oblique bars (SVR sediment transport, θ^0=10°), and (d) Up-current oblique bars (CWS sediment transport, θ^0=10°). Plus-symbol (+), wavelength at the equilibrium state (λ_{be}) as a function of the preexisting wavelength (λ_{ini}). Vertical line (error bar), range of wavelength λ_b as a function of λ_{ini}. Dashed line, slope 1:1 line. Grey horizontal line, equilibrium wavelength λ_{be} obtained from free instability (Table 3). Grey surface, range of wavelength λ_b obtained from free instability (Table 3).

Starting from pre-existing cusps

Default model settings, changing cusp spacing

In this part the initial conditions have been changed by assuming that large beach cusps are present at the initial time, but with a small amplitude, retaining the amplitude of the perturbation used in the previous sections (5 mm). Figure 10a shows an example of this initial topography, where the cusp wave length is λ_{ini}=30 m. The initial wavelength has been set as $0<\lambda_{ini}<80$ m, and three different model settings have been used, corresponding to the three kinds of instabilities shown in Figure 9.

Depending on the experiments, the initial wave length is preserved for a larger or shorter duration, but it is conserved for the entire evolution only if the initial wave length is close to the equilibrium wavelength obtained from a free instability (Fig. 10b, d). For instance, Figure 10b shows that, for α_{SVR} and normal waves, the initial wavelength is kept if $30\leq\lambda_{ini}\leq40$ m (from free instability, at the equilibrium, $\lambda_b=\lambda_{be}$=35 m), and for oblique waves (Fig. 10c), no merging/splitting is observed if $25\leq\lambda_{ini}\leq35$ m (λ_{be}=31 m from free instability). For α_0, the initial wavelength is preserved if $\lambda_{ini}\geq50$ m (λ_{be}=100 m from free instability).

In general the system reorganizes into a bar system with a wavelength close to the one observed for free instability (i.e. grey surface in Fig. 10b, d), but the equilibrium wave length is not necessarily the same as the free instability one (grey horizontal line). In particular, for α_0 the wavelength for free instability (100 m) is never reached, and the new equilibrium value can be up to half this length (for λ_{ini}=50 m, λ_{be}=50 m)These experiments reveal the sensitivity of the instability characteristics depending on the initial conditions and show that pre-existing cusps can alter the self-organization of the surf zone. For instance, the LBC can force the wave length of surf zone bars. However, by imposing a small wavelength in the pre-existing patterns, i.e. by considering the small beach cusps of λ_c~10 m sometimes observed at Trafalgar Beach, merging is observed and bar characteristics depend less on the pre-existing cusps.

Model settings leading to stability, λ_c=30 m

The model settings leading to stability used in the previous section were applied to the case of pre-existing large cusps. The amplitude of the cusps was set to 10 cm and the wave length to 30 m. Prior to each experiment a hydrodynamical equilibrium state was obtained by disconnecting the sediment transport. Changes in selected settings with respect to the default case were the incident wave angle (1) θ^0=1° and (2) θ^0=15°; the shore beach slope (3) β_0=0.15; and the sediment transport (4) $\alpha=\alpha_0$. The damping of the initial features was eventually observed in all the experiments, but the time necessary, as well as the transient dynamics to reach a flat topography, differed.

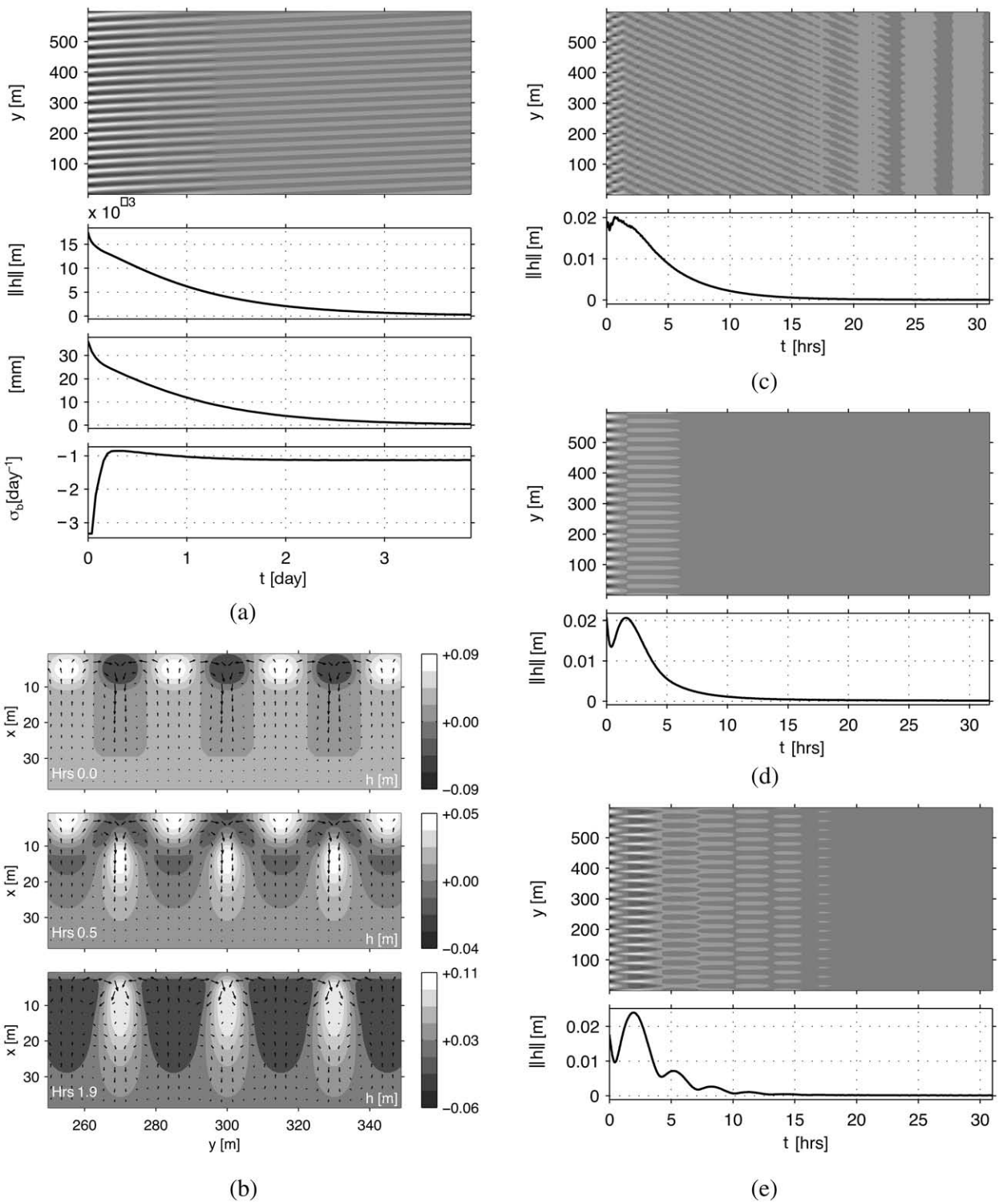

FIG. 11. – Damping of pre-existing cusps. (a) Time series for θ^0=1°: h(x=5 m,y), |h|, the Fourier coefficient of the predominant mode and σ_b. (b) Snapshots of the bed perturbation h and current vectors for $\alpha=\alpha_0$. (c-e) Time series for (c) θ^0=15°, (d) β_0=0.15, (e) $\alpha=\alpha_0$: h(x=5 m,y) and |h|.

Decay occurred more slowly in the experiment where θ^0=1° (Fig. 11a). This experiment was also the less dynamical, as only one mode was present during the evolution, corresponding to the initial wavelength. This mode amplitude decreased monotonically, so we obtained a clear representation of the corresponding growth rate σ_b (which was negative in this case). The stronger decrease occurred at the initial time, where σ_b~ -3 day^{-1}. Then the bars reorganized so that the new system was less rapidly damped. The growth rate

was constant ($\sigma_b \sim$ -1 day^{-1}) until the initial features disappeared after more than 3 days of morphological evolution.

The global processes were much faster in the other experiments, as after 1 day of morphological evolution the beach was flat and stable (Fig. 11c, e). As the oscillations in the bar norm plots |h| show, the processes were more complex, in particular in experiment (4) ($\alpha=\alpha_0$). These oscillations were also observed in the Fourier coefficient, so a realistic growth rate cannot be computed as it ranges from strong negative to positive values. The snapshots of the bed level perturbation (Fig. 11b) illustrate the complex behaviours occurring in experiment (4). The damping of the initial features was observed in the first few minutes, but they increased again and became higher after two hours, being in anti-phase with the pre-existing cusps. They were fully flattened after 20 hours of evolution.

This experiment illustrates the complexity of the surf zone processes and therefore points out the difficulty of parametrizing these processes in swash zone models. Though the 2DH model predicts stability for particular settings, and pre-existing feature will eventually be damped, the transient states can be complex and we can observe strong dynamical changes in the first minutes of the morphological evolution and the growth of these feature at some times. These changes occur in the time scale of the cusp formation predicted by the models of Coco *et al.* (2000) and Dodd *et al.* (2008). This adds complication to the understanding of cusp dynamics.

Result overview

For characteristic conditions favouring the emergence of the LBC, we found three kinds of instabilities, depending on the incident wave angle and on the sediment transport parameterization. For strictly normal waves, transverse bars emerge with wavelength of ~20-30 m using the Soulsby and Van Rijn (SVR) sediment transport formula. As soon as wave obliquity is imposed, the transverse bar mode does not appear, but two other modes can emerge. They are oblique bars oriented down-current or up-current, depending on whether the SVR formula or a constant wave stirring is chosen, respectively. While the down-current bars (wavelength of ~20-40 m) can appear for very weak obliquity and disappear for large obliquity, the up-current bars (wavelength of ~50-120 m) grow faster for a stronger ambient alongshore current (>0.7 ms^{-1}). The transverse bar mode grows faster (i.e. growth rate ~5 day^{-1}) than the oblique bar modes (growth rate ~2 day^{-1}). Further, the instability is favoured by a larger incident wave height and wave period, and by smaller beach slope and smaller grain size. The stability of the beach is obtained for large slope, for some particular values of the incident wave angle using the SVR transport formula, for small wave angles using a constant wave stirring, or by simply increasing the bedslope transport coefficient. With these model settings, the LBC are expected to eventually damp in the surf zone. However, in some cases, complex transient states are found, sometimes showing the growth of the features in the initial step of the morphological evolution (i.e. after some minutes). These transient behaviours need further attention as they occur for the time scale of the cusp formation.

In general, from these self-organization experiments (starting from a random perturbed alongshore uniform topography), an equilibrium beach state is reached, and is characterized by a bar wavelength that becomes constant in time. We found that this solution depends on the initial conditions, and in particular on the initial wavelength of pre-existing bedforms. For initial wavelengths in the neighbourhood of the one obtained from free instability, the initial wavelength is conserved. Thus, for the range of the LBC wavelength observed at Trafalgar Beach, merging/splitting is not necessarily expected to occur in the surf zone. However, if the initial wavelength is close to the small cusp wavelength (~10 m), the model predicts reorganization and merging of the cusps in the surf zone.

CONCLUSIONS

Beach cusps are rhythmic systems that feature a periodic undulation of the shoreline with a period (wavelength) ranging from centimetres to tens of metres. Based on field observations at the Trafalgar sandy beach (Cádiz, Spain) a distinction within the beach cusps is established. The 'large beach cusps' ('LBC', wavelength ~30 m) are differentiated from the smaller cusps (wavelength <20 m) in several aspects. Apart from the wavelength, the difference consists in their location (the small cusps appear in the upper beach while the LBC appear in the overall intertidal zone), and in their cross-shore extent (the LBC have a larger protruding distance [up to 50 m] than the small cusps [<5 m], so they alternately stand in the swash and in the inner surf zone due to tidal sea level changes). Moreover, the LBC are notable in that they sometimes present an oblique orientation with respect to the mean shoreline, and they sometimes migrate alongshore. These distinctions suggest that different mechanisms could be at the origin of the formation of these cusps.

Previous studies show that beach cusps appear from swash zone mechanisms and that the surf zone processes are exclusively destructive. However, by using a 2DH surf zone morphodynamical numerical model that neglects the swash zone processes and the changes in tide level, we see that inner surf zone processes do not always destroy the cusps but can in fact reinforce them. More generally, in the conditions leading to the presence of LBC the surf zone can be morphodynamically unstable, with the bars emerging from this instability having characteristics similar to the LBC. Therefore, LBC could also be formed by surf zone processes and an analogy with the megacusps can be made. Further-

more, surf zone models usually neglect swash zone processes and the presence of beach cusps, but we show that cusps can trigger the formation of transverse/oblique bars by forcing the wavelength of the surf zone features. Thus, the dynamics of beach cusps appears to be closely related to the interaction between surf and swash zones.

Although this study reveals the possibility of the growth of large beach cusps in the surf zone from the results of a 2DH numerical model, the lack of field measurements does not allow direct observation of the growth or the decay of these cusps in the surf zone. First, Argus images are not accurate enough to measure morphological behaviour in the inner surf zone; for instance the strong undertow occurring in the channels can be confounded with breaking over the crests. Second, a validation of the model would need hydrodynamical measurements. Nevertheless, in spite of all these limitations, the present study suggests that beach cusp dynamics does not rely only on swash zone processes, but involve a complex interaction between swash and surf zones that should be explored in future research.

ACKNOWLEDGEMENTS

The work of R. Garnier was supported by the University of Nottingham and is part of the Spanish Government project under contract CTM2006-08875. The Spanish Ministry of Science and Education (Project BORRASCAS CTM2005-06583) and the Junta de Andalucía (Projects P05-RNM-968 and P06-RNM-1573) funded part of this research. Their support is gratefully acknowledged. The authors also thank Prof. Holman for the Argus hints.

REFERENCES

Aarninkhof, S. and R. Holman. – 1999. Argus video-based monitoring of the nearshore zone: a tool for both nearshore science and coastal zone management. *Backscatter*, 10(2): 8-11.

Almar, R., G. Coco, K. Bryan, D. Huntley, A. Short, and N. Senechal. – 2008. Video observations of beach cusp morphodynamics. *Mar. Geol.*, 254: 216-223.

Booij, N., R.C. Ris and L.H. Holthuijsen. – 1999. A third-generation wave model for coastal regions: 1. Model description and validation. *J. Geophys. Res.*, 104(C4): 7649-7666.

Caballeria, M., G. Coco, A. Falqués and D.A. Huntley. – 2002. Self-organization mechanisms for the formation of nearshore crescentic and transverse sand bars. *J. Fluid Mech.*, 465: 379-410.

Calvete, D., N. Dodd, A. Falqués and S.M. van Leeuwen. – 2005. Morphological development of rip channel systems: Normal and near normal wave incidence. *J. Geophys. Res.*, 110(C10006), doi:10.1029/2004JC002803.

Castelle, B., P. Bonneton, H. Dupuis and N. Senechal. – 2007. Double bar beach dynamics on the high-energy meso-macrotidal french Aquitanian coast: a review. *Mar. Geol.*, 245: 141-159.

Ciriano, Y., G. Coco, K. Bryan and S. Elgar. – 2005. Field observations of infragravity motions in the swash zone and beach cusp evolution. *J. Geophys. Res.*, 110(C02018), doi:10.1029/2004JC002485.

Coco, G., T. J. O'Hare, and D. A. Huntley. – 1999. Beach cusps: a comparison of data and theories for their formation. *J. Coastal Res.*, 15(3): 741-749.

Coco, G., D.A. Huntley and T.J. O'Hare. – 2000. Investigation of a self-organization model for beach cusp formation and development. *J. Geophys. Res.*, 105(C9): 21,991-22,002.

Coco, G., T.K. Burnet, B.T. Werner and S. Elgar. – 2003. Test of self-organization in beach cusp formation. *J. Geophys. Res.*, 108(C33101), doi:10.1029/2002JC001496.

Coco, G., T.K. Burnet, B.T. Werner and S. Elgar. – 2004. The role of tides in beach cusp development. *J. Geophys. Res.*, 109(C04011), doi:10.1029/2003JC002154.

Dodd, N., A. Stoker, D. Calvete and A. Sriariyawat. – 2008. On beach cusp formation. *J. Fluid Mech.*, 597: 145-169.

Falqués, A., G. Coco, and D. A. Huntley. – 2000. A mechanism for the generation of wave-driven rhythmic patterns in the surf zone. *J. Geophys. Res.*, 105(C10): 24,071-24,088.

Garnier, R., D. Calvete, A. Falqués and M. Caballeria. – 2006. Generation and nonlinear evolution of shore-oblique/transverse sand bars. *J. Fluid Mech.*, 567: 327-360.

Garnier, R., D. Calvete, A. Falqués and N. Dodd. – 2008. Modelling the formation and the long-term behaviour of rip channel systems from the deformation of a longshore bar. *J. Geophys. Res.*, 113(C07053), doi:10.1029/2007JC004632.

Guza, R.T. and A. Bowen. – 1975 On the amplitude of beach cusps. *J. Geophys. Res.*, 86: 4125-4131.

Guza, R.T. and D. Inman. – 1975. Edge waves and beach cusps. *J. Geophys. Res.*, 80(21): 2997-3012.

Holland, K.T. – 1998. Beach cusp formation and spacings at Duck, USA. *Cont. Shelf Res.*, 18: 1081-1098.

Holland, K.T. and R.A. Holman. – 1996. Field observations of beach cusps and swash motions. *Mar. Geol.*, 134: 77-93.

Holland, K.T., R.A. Holman, T.C. Lippmann, J. Stanley and N. Plant. – 1997. Practical use of video imagery in nearshore oceanographic field studies. *IEEE J. Ocean. Eng.*, 22(1): 81-92.

Holman, R.A. and J. Stanley. – 2007. The history and technical capabilities of Argus. *Coastal Eng.*, 54(6-7): 477-491.

Inman, D.L. and R.T. Guza. – 1982. The origin of swash cusps on beaches. *Mar. Geol.*, 49: 133-148.

Johnson, B. and J. Smith. – 2008. A two-scale approach to nearshore sediment transport modeling. In: J.M. Smith (ed.), *Coastal Eng. 2008*, pp. 1671-1683. World Sci., Singapore.

Masselink, G. and C.B. Pattiaratchi. – 1998. Morphological evolution of beach cusp morphology and associated swash circulation patterns. *Mar. Geol.*, 146: 93-113.

Masselink, G. and A.D. Short. – 1993. The effect of the tide range on beach morphodynamics: a conceptual model. *J. Coastal Res.*, 9: 785-800.

Masselink, G., B.J. Hegge and C.B. Pattiaratchi. – 1997. Beach cusp morphodynamics. *Earth Surf. Proc. Land.*, 22: 1139-1155.

Masselink, G., P. Russell, G. Coco and D.A. Huntley. – 2004. Test of edge wave forcing during formation of rhythmic beach morphology. *J. Geophys. Res.*, 109(C06003), doi:10.1029/2004JC002339.

Ortega-Sánchez, M., M.A. Losada and A. Baquerizo. – 2003. On the development of large-scale features on a semi-reflective beach: Carchuna beach, southern Spain. *Mar. Geol.*, 198: 209-223.

Ortega-Sánchez, M., S. Fachin, F. Sancho and M.A. Losada. – 2008. Relation between beachface morphology and wave climate at Trafalgar beach (Cádiz, Spain). *Geomorphology*, 99: 171-185.

Ribas, F., A. Falqués and A. Montoto. – 2003. Nearshore oblique sand bars. *J. Geophys. Res.*, 108(C43119), doi:10.1029/2001JC000985.

Short, A.D. – 1999. *Handbook of Beach and Shoreface Morphodynamics*. Wiley, Chichester.

Soulsby, R.L. – 1997. *Dynamics of Marine Sands*, Thomas Telford, London, U.K.

van Leeuwen, S.M., N. Dodd, D. Calvete and A. Falqués. – 2006. Physics of nearshore bed pattern formation under regular or random waves. *J. Geophys. Res.*, 111(F01023), doi:10.1029/2005JF000360.

Werner, B.T. and T.M. Fink. – 1993. Beach cusps as self-organized patterns, *Science*, 260: 968-971.

Wright, L.D. and A.D. Short. – 1984. Morphodynamic variability of surf zones and beaches: A synthesis. *Mar. Geol.*, *56*: 93-118.

Scient. ed.: J. Guillén.
Received June 10, 2009. Accepted November 19, 2009.
Published online May 20, 2010.